ISSN 1674-1056
http://cpb.iphy.ac.cn
http://iopscience.iop.org/cpb
中国物理 B
Chinese Physics
Chinese Physics B

Broadband achromatic phase retarder based onmetal-multilayer dielectric grating

Na Li(李娜), Wei-Jin Kong(孔伟金), Feng Xia(夏峰), Mao-Jin Yun(云茂金)
Citation: Chin. Phys. B . 2018, 27(5): 054202. **doi:** 10.1088/1674-1056/27/5/054202

Journal homepage: http://cpb.iphy.ac.cn; http://iopscience.iop.org/cpb

What follows is a list of articles you may be interested in

Diurnal cooling for continuous thermal sources under direct subtropical sunlight produced by quasi-Cantor structure

Jia-Ye Wu(吴嘉野), Yuan-Zhi Gong(龚远志), Pei-Ran Huang(黄培然), Gen-Jun Ma(马根骏), Qiao-Feng Dai(戴峭峰)
Chin. Phys. B . 2017, 26(10): 104201. **doi:** 10.1088/1674-1056/26/10/104201

Simple and universal method in designs of high-efficiency diffractive optical elements for spectrum separation and beam concentration

Wen-Qi Xu(徐文琪), Dong-Feng Lin(林冬风), Xin Xu(许信), Jia-Sheng Ye(叶佳声), Xin-Ke Wang(王新柯), Sheng-Fei Feng(冯胜飞), Wen-Feng Sun(孙文峰), Peng Han(韩鹏), Yan Zhang(张岩), Qing-Bo Meng(孟庆波), Guo-Zhen Yang(杨国桢)
Chin. Phys. B . 2017, 26(7): 074202. **doi:** 10.1088/1674-1056/26/7/074202

Realizing high photovoltaic efficiency with parallel multijunction solar cells based on spectrum-splitting and -concentrating diffractive optical element

Wang Jin-Ze, Huang Qing-Li, Xu Xin, Quan Bao-Gang, Luo Jian-Heng, Zhang Yan, Ye Jia-Sheng, Li Dong-Mei, Meng Qing-Bo, Yang Guo-Zhen
Chin. Phys. B . 2015, 24(5): 054201. **doi:** 10.1088/1674-1056/24/5/054201

Design optimization of highly efficient spectrum-splitting and beam-concentrating diffractive optical element for lateral multijunction solar cells

Wang Jin-Ze, Ye Jia-Sheng, Huang Qing-Li, Xu Xin, Li Dong-Mei, Meng Qing-Bo, Yang Guo-Zhen
Chin. Phys. B . 2014, 23(4): 044211. **doi:** 10.1088/1674-1056/23/4/044211

A cost-effective structure of a centralized-light-source WDM-PON utilizing inverse-duobinary-RZ downstream and DPSK upstream

Chen Long-Quan, Qiao Yao-Jun, Ji Yue-Feng
Chin. Phys. B . 2013, 22(5): 054201. **doi:** 10.1088/1674-1056/22/5/054201

Broadband achromatic phase retarder based on metal-multilayer dielectric grating*

Na Li(李娜)[1,2], Wei-Jin Kong(孔伟金)[1,3,†], Feng Xia(夏峰)[1], and Mao-Jin Yun(云茂金)[1,3]

[1] College of Physics, Qingdao University, Qingdao 266071, China
[2] Qingdao Laoshan No. 2 Middle School, Qingdao 266071, China
[3] Key Laboratory of Photonics Materials and Technology in Universities of Shandong, Qingdao University, Qingdao 266071, China

(Received 8 November 2017; revised manuscript received 24 January 2018; published online 26 April 2018)

A new achromatic phase retarder based on a metal-multilayer dielectric grating structure is designed using the rigorous coupled wave analysis method and the genetic algorithm. The optimized phase retarder can maintain phase retardation around 90° from 900 nm to 1200 nm, and the maximum deviation is less than 4.5% while the diffraction efficiencies of TE and TM waves are both higher than 95%. Numerical analysis shows the designed phase retarder has a high fabrication tolerance of groove depth, duty cycle and incident angle. This achromatic phase retarder is simple in design and stable in performance, and can be widely used in optical systems.

Keywords: achromatic phase retarder, metal-multilayer dielectric grating, rigorous coupled wave analysis (RCWA), genetic algorithm (GA)

PACS: 42.15.Eq, 42.40.Lx, 42.79.Dj, 42.87.Bg **DOI:** 10.1088/1674-1056/27/5/054202

1. Introduction

The phase retarder is one of the most common elements in an optical system, which can be divided into the quarter-wave plate, the half-wave plate and the full-wave plate. Conventional phase retarders usually use birefringent material,[1] multilayer dielectric film[2] and liquid crystal.[3] Traditional phase retarders generally can be used only at a specific wavelength, since the phase retardation strongly depends on the wavelength. However, achromatic phase retarders greatly reduce the wavelength dependence of phase retardation, which can realize the modulation of polarized light in a wide spectrum. In recent years, the resonant regime of achromatic phase retarders has attracted more attention, where the grating period is close to the incidence wavelength. Kikuta *et al.*[4] first achieved an achromatic quarter-wave plate by utilizing the dispersion of effective refractive indices theoretically. According to this method, Nordin and Deguzman[5,6] realized an element functioning as an achromatic quarter-wave plate in mid-infrared wavelength. Bokor *et al.*[7] designed an achromatic quarter-wave plate from 470 nm to 630 nm. Yi[8] designed a sub-wavelength grating achromatic phase retarder on fused silica at 400–800 nm visible light. Kang *et al.*[9] proposed a combination of four sub-wavelength structured gratings used as an achromatic quarter-wave plate, which was applied to MWIR (3–5 μm) & LWIR (8–12 μm) bandwidths based on effective medium theory and optimization algorithms. Yamada *et al.*[10] fabricated an achromatic wave plate by forming a sub-wavelength grating on chalcogenide glass by using direct imprint lithography, with the phase retardation of the element reaching around 30° at 8.5–10.5 μm wavelength.

In this paper, an achromatic phase retarder based on the metal-multilayer grating (MMDG)[11–14] is designed. The designed phase retarder can be used at wavelengths ranging from 900 nm to 1200 nm, where its retardation can maintain about $90° \pm 4°$, while the diffraction efficiencies of TE and TM waves are higher than 95%. Furthermore, the performance modulation of the grating parameters on the phase retardation is analyzed.

2. Theoretical model

As shown in Fig. 1, the structure of the MMDG used for the achromatic phase retarder is composed of a surface relief structure, a residual layer, a double layer dielectric and a metal layer. The parameters of the MMDG are denoted as follows: D, f, Λ, θ and tr represent the groove depth, duty cycle, the period of grating, incident angle and thickness of residual layer. t_1, t_2, t_3 refer to the thickness of SiO_2 layer, HfO_2 layer and Ag layer, respectively.

Given that the wavelength of incident light is comparable to the grating period, the designed phase retarder reflects the TE and TM waves in the 0th order, thus the scalar analysis is no longer applicable. Therefore, the rigorous coupled wave analysis (RCWA) method does not hold true for calculating the diffraction efficiency of the MMDG structure.[15] The RCWA method enables the exact solution of the system of Maxwell equations built by the electromagnetic field from a grating.[16,17] With the enhanced transmission method to improve the traditional coupled wave analysis, the numerical in-

*Project supported by the National Natural Science Foundation of China (Grant No. 11274188)
†Corresponding author. E-mail: kwjsd@163.com
© 2018 Chinese Physical Society and IOP Publishing Ltd

stability problem encountered in the process of calculating the etched grating is well solved.[18,19]

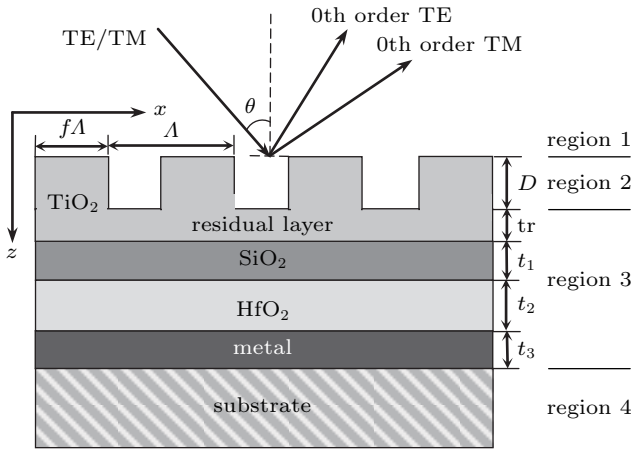


Fig. 1. Schematic diagram of the metal-multilayer dielectric grating used as an achromatic phase retarder with surface-relief, double-layer dielectric and metal-layer gratings.

As depicted in Fig. 1, the grating lies in the xz plane. A grating can be divided into four regions. Regions 1 and 4 are the input region and output region, respectively; region 2 is the rectangle grating region; and region 3 is the multilayer film region. Here, a TE polarization plane wave is considered as incident light. In the grating region: $0 < Z < D$, the normalized electric field and the magnetic field can be given as follows:

$$\begin{aligned} E_{l,\mathrm{g}y} &= \sum_i S_{l,yi}(z)\exp(-\mathrm{j}k_{xi}x), \\ H_{l,\mathrm{g}x} &= -\mathrm{j}(\varepsilon_\circ/\mu_\circ)^{1/2}\sum_i U_{l,xi}(z)\exp(-\mathrm{j}k_{xi}x). \end{aligned} \tag{1}$$

Meanwhile, the general solution of differential equation can be expressed as follows:

$$\begin{aligned} S_{l,y}(z) &= \sum_{m=1}^{n} w_{l,i,m}\{c^{+}_{l,m}\exp[-k_0 q_{l,m}(z-D_l+d_l)] \\ &\quad + c^{-}_{l,m}\exp[k_0 q_{l,m}(z-D_l)]\}, \\ U_{l,x}(z) &= \sum_{m=1}^{n} v_{l,i,m}\{-c^{+}_{l,m}\exp(z-D_l+d_l) \\ &\quad + c^{-}_{l,m}\exp[k_0 q_{l,m}(z-D_l)]\}. \end{aligned} \tag{2}$$

By substituting the above solution into each layer of electromagnetic field tangential continuity conditions recursively, the amplitude coefficient of the reflected diffraction wave $\boldsymbol{R_i}$ is obtained. Then the diffraction efficiency of reflection is expressed as

$$DE_{ri} = R_i R_i^{*}\,\mathrm{Re}(k_{\mathrm{I},zi}/k_0 n_{\mathrm{I}}\cos\theta), \tag{3}$$

where $\boldsymbol{k}_{\mathrm{I},zi}$, $\boldsymbol{k}_0$ and n_{I} are the z component of the wavevector of the diffracted light in the incident area, the wave vector of the incident light wave and the refraction index of the incident area, respectively.

Then the phases of TE and TM waves are obtained with the diffraction amplitude coefficient as follows:

$$\varphi_{\mathrm{TE}} = \arg(\boldsymbol{R}_{\mathrm{TE}}), \quad \varphi_{\mathrm{TM}} = \arg(\boldsymbol{R}_{\mathrm{TM}}), \tag{4}$$

where $\boldsymbol{R}_{\mathrm{TE}}$ and $\boldsymbol{R}_{\mathrm{TM}}$ are the 0th reflected diffraction wave amplitude coefficient of the TE and TM waves, respectively.

Thus, the phase retardation of TE and TM waves is obtained as follows:

$$\Delta\varphi = \varphi_{\mathrm{TE}} - \varphi_{\mathrm{TM}}. \tag{5}$$

3. Design and optimization

Here, a certain layer below the surface relief structure was not etched in the fabrication process. The residual layer was regarded as a waveguide exerting significant influence on diffraction efficiency.[20] Therefore, TiO_2 ($n = 2.3$) was chosen as the surface relief and residual layer material because of its high refractive index over a broad bandwidth. Meanwhile, the substrate was made of fused silica.

As can be seen in Fig. 1, SiO_2 ($n_1 = 1.46$) and HfO_2 ($n_2 = 1.96$) layers make a simple double layer structure which makes fabrication more feasible.[21] Ag layer ($n_3 = 0.2309$–7.1452i at 1053 nm) performs as a highly reflective mirror, and thus it can be used as a metal layer to achieve broadband because of its low absorption ratio.

With the metal layer made of Ag, the number of dielectric layers in the MMDG is reduced to only two, meanwhile providing a high reflection efficiency.[22] The MMDG structure also presents a high laser-induced damage threshold over a broad wavelength.[23] Moreover, the fabricated MMDG can efficiently separate the incident waves through polarization. Due to the sub-wavelength structure of the MMDG and the different boundary conditions of the electromagnetic wave, the TE and TM waves exhibit phase displacement while propagating in the MMDG. This observation implies that the TE and TM waves are separated during MMDG modulation.

In order to obtain a smaller deviation of phase retardation as well as higher diffraction efficiency by optimizing MMDG parameters, here a merit function (MF) is defined as

$$\mathrm{MF} = \mathrm{mean}[\mathrm{abs}(90^\circ - \Delta\varphi)], \tag{6}$$

where MF represents the best merit. By this definition, the smaller the value, the smaller the deviation of phase retardation is and the better the performance of designed phase retarder.

In this design, a genetic algorithm (GA)[24] is used to optimize the parameters of the given MMDG structure. To obtain the optimal structure of the achromatic phase retarder, parameters such as $\{D,\ f,\ \Lambda,\ \theta,\ \mathrm{tr},\ t_1,\ t_2,\ t_3\}$ are considered. The minimum and maximum values of these parameters are set to be $\{200,\ 0.1,\ 50,\ 0,\ 0,\ 50,\ 50,\ 50\}$ and $\{400,\ 0.5,\ 350,\ 60,\ 50,\ 150,\ 150,\ 150\}$, respectively. In the GA, a set of values

is randomly selected as the initial population of individual solutions, then the GA works by iteratively using three genetic operators (i.e., select, crossover, and mutation) to change the population based on the merit function. Therefore, by maximizing the merit function, one can find optimal parameters for the achromatic phase retarder.

4. Simulation results and discussion

4.1. Parameters of the MMDG

We optimize the given structure by using the merit function over the range of 900–1200 nm. The corresponding parameters of the designed phase retarder are listed in Table 1.

Table 1. Optimized parameters of the MMDG.

D/nm	f	Λ/nm	$\theta/(^\circ)$	tr/nm	t_1, t_2, t_3/nm
347	0.3	248	30	18	92,145,87

According to the parameters in Table 1, the characteristics spectrum of the designed phase retarder is plotted in Fig. 2, in a wavelength range from 900 nm to 1200 nm, which shows the curves of phase retardation and diffraction efficiency versus wavelength, respectively.

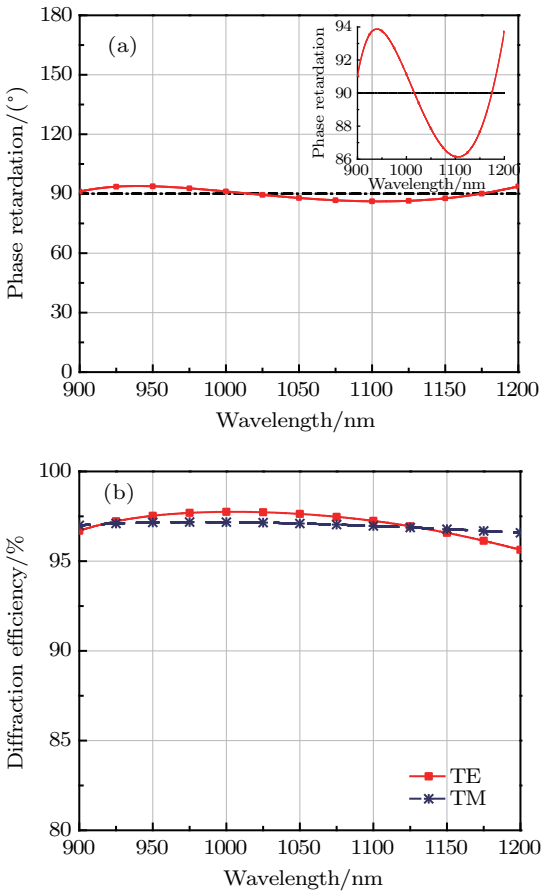


Fig. 2. (color online) Designed MMDG characteristics spectrum with TE and TM waves, showing wavelength-dependent (a) phase retardation and (b) diffraction efficiency.

The phase retardation and diffraction efficiency calculated by RCWA are shown in Fig. 2. As can be seen in Fig. 2(a), the phase retardation of the MMDG, in the case of TE and TM waves in the 0th order, is about 90°, in which the deviation is less than 4°. Figure 2(b) shows that the diffraction efficiencies of TE and TM waves in the 0th order are both higher than 95%, given that the wavelength ranges from 900 nm to 1200 nm. These plots suggest that our designed phase retarder has a favorable performance over the given wavelength range.

4.2. Fabrication tolerance analysis of the MMDG

The fabricated grating normally has a minor difference from the designed structure because of the complexity of the production. It is especially necessary that the fabrication deviation should not substantively influence the characteristics of the grating. Thus, favorable fabrication tolerance is extraordinarily necessary for grating fabrication.[25] To show how the deviation of groove depth, duty cycle and incident angle affect phase retardation intuitively, the three-dimensional graphs of the phase retardation with TE and TM waves in the 0th order are depicted in Fig. 3.

Figure 3 represents the dependence of fabrication tolerance on wavelength and grating parameters. It shows a smoothly curved plane of phase retardation in a wavelength range from 900 nm to 1200 nm. With the groove depth changing from 330 nm to 360 nm, the duty cycle changing from 0.26 to 0.34 and the incident angle varying from 25° to 35°, the phase retardations of TE and TM waves are maintained at 90°, while its deviation is about 10°.

Figure 4 shows how the deviations of groove depth, duty cycle and incident angle affect the phase retardations of the TE and TM waves, respectively. The error analysis of the effect on the MMDG is as follows.

According to the current fabrication techniques, controlling the grating groove depth is very difficult, where the error is usually controlled at $\Delta D = \pm 10$ nm,[26] so we calculate the errors at $D_1 = D - \Delta D = 337$ nm and $D_2 = D + \Delta D = 357$ nm. The effects of deviation of groove depth on phase retardation are given in Fig. 4(a), showing that the phase retardations of the TE and TM waves can be maintained in a range from 85° to 98°.

Figure 4(b) shows the deviations of duty cycle effected on phase retardations of TE and TM waves in the 0th order, with the error controlled at ±10 nm.[27] The duty cycle is $f = 0.3 \pm 0.04$, for a grating with a period of 248 nm. The calculated minimum and maximum values of the phase retardation are 83° and 104°, respectively. It means that the duty cycle is a very sensitive factor for the phase delay.

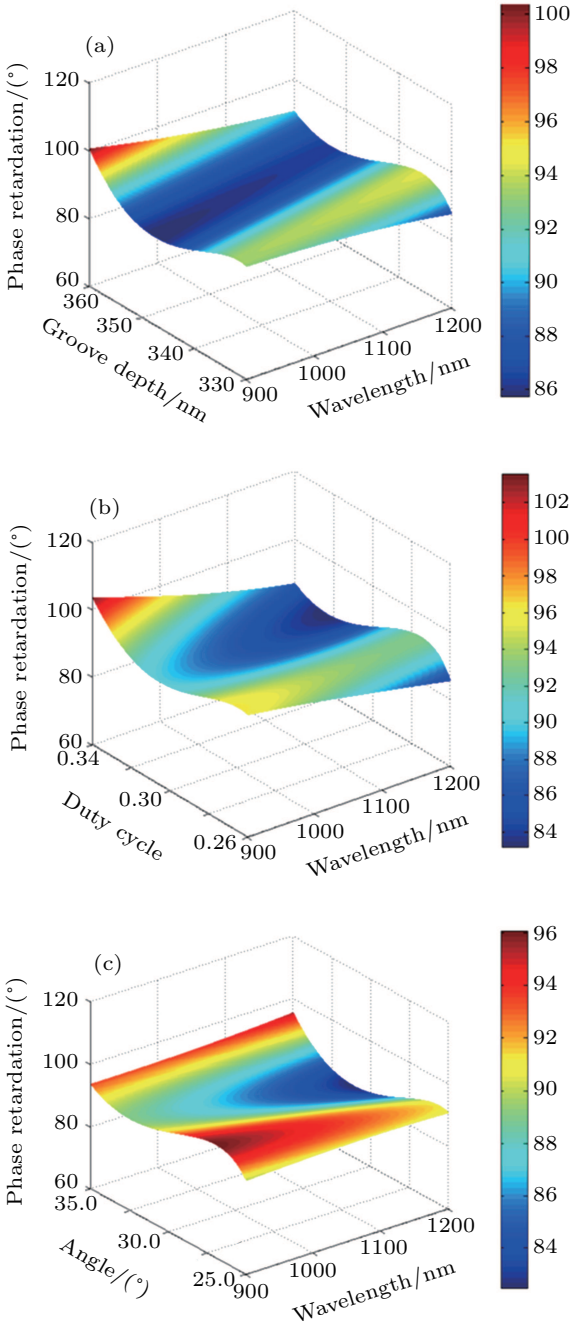


Fig. 3. (color online) Dependence of fabrication tolerance on (a) groove depth, (b) duty cycle, (c) incident angle in a wavelength range of 900–1200 nm.

Furthermore, when the device is employed, the installation deviation will cause the incident angle to deviate from 30° to the grating surface ($\theta \neq 30°$). Given $\Delta\theta = \pm 5°$, we calculate the deviations at $\theta_1 = 25°$ and $\theta_2 = 35°$, the effects of deviation of incident angle on phase retardations of the TE and TM waves in the 0th order are given in Fig. 4(c), showing that the phase retardation deviation is kept at 10°.

As can be seen in Fig. 4, the deviations of the groove depth, duty cycle and incident angle do not change the performance of the optimized phase retarder much. Meanwhile, the optimized groove depth and duty cycle are achievable by the current fabrication techniques. A large incident angle range can fulfill bandwidth of more than 300 nm with phase retardation maintained around 90° and diffraction efficiency exceeding 95% for TE and TM waves in the 0th order. The analysis shows that the designed phase retarder has a larger fabrication tolerance for groove depth, duty cycle and incident angle in a wavelength range from 900 nm to 1200 nm.

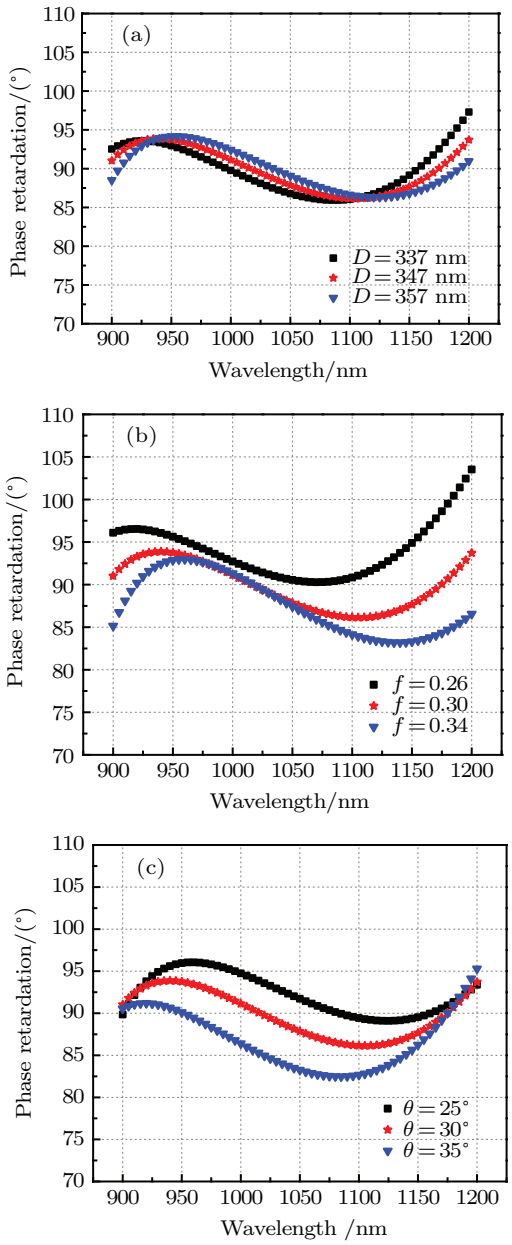


Fig. 4. (color online) Effects of deviation of (a) groove depth, (b) duty cycle, and (c) incident angle on phase retardations of TE and TM waves.

According to the previous analysis, the considerable fabrication tolerance has provided a perfect guarantee for the grating fabrication and fine characteristics in an optical system.

5. Conclusions

In this paper, a new achromatic phase retarder based on MMDG is designed theoretically by RCWA and optimized by GA. Numerical results show that the designed phase retarder

at 900–1200 nm exhibits high reflected diffraction efficiency and a small deviation of phase retardation, with diffraction efficiency higher than 95% for TE and TM waves in the 0th order over 300 nm bandwidth, while phase retardation deviation is less than 4°. Fabrication deviation analysis indicates that the designed MMDG has favorable tolerance and can be easily fabricated. The results suggest that the optimized MMDG has potential applications as the phase retarder in optical fibers, laser systems and optical elements.

References

[1] Veiras F E, Raffa G, CaréD, Perez L I and Garea M T 2014 *Rev. Sci. Instrum.* **85** 033109
[2] Apfel J H 1982 *Appl. Opt.* **21** 733
[3] Abuleil M and Abdulhalim J I 2014 *Opt. Lett.* **39** 5487
[4] Kikuta H, Ohira Y and Iwata K 1997 *Appl. Opt.* **36** 1566
[5] Nordin G P and Deguzman P C 1999 *Opt. Express* **5** 163
[6] Deguzman P C and Nordin G P 2000 *Appl. Opt.* **40** 5731
[7] Bokor N, Shechter R, Davidson N, Friesem A A and Hasman E 2001 *Appl. Opt.* **40** 2076
[8] Yi D E, Yan Y B, Liu H T, Lu S and Jin G F 2003 *Opt. Commun.* **227** 49
[9] Kang G, Tan Q, Wang X and Jin G 2010 *Opt. Express* **18** 1695
[10] Yamada I, Yamashita1 N, Tani1 K, Einishi T, Saito M, Fukumi K and Nishii J 2012 *Appl. Phys. Express* **5** 072601
[11] Canova F, Uteza O, Chambaret J P, Flury M, Tonchev S, Fechner R and Parriaux O 2007 *Opt. Express* **15** 15324
[12] Wang J, Jin Y, Ma J, Sun T and Jing X 2010 *Appl. Opt.* **49** 2969
[13] Neauport J, Bonod N, Hocquet S, Palmier S and Dupuy G 2010 *Opt. Express* **18** 23776
[14] Flury M, Tonchev S, Fechner R, Schindler A and Parriaux O 2007 *J. Eur. Opt. Soc. Rapid* **2** 07024
[15] Moharam M G, Gaylord T K and Magnusson R 1980 *Opt. Soc. Am.* **70** 300
[16] Moharam M G and Gaylord T K 1981 *Opt. Soc. Am.* **71** 811
[17] Moharam M G and Gaylord T K 1981 *Appl. Opt.* **20** 240
[18] Moharam M G, Grann E B and Pommet D A 1995 *J. Opt. Soc. Am.* **12** 1068
[19] Kong W J, Wang S H, Wei S J, Yun M J, Zhang W F, Wang X J and Zhang M M 2011 *Acta Phys. Sin.* **60** 114214 (in Chinese)
[20] Wang J P, Jin Y X, Ma J Y, Shao J D and Fan Z X 2010 *Acta Phys. Sin.* **59** 3199 (in Chinese)
[21] You C L, Kong W J, Cao K H, Wang Z, Wang W X, Yun M J, Liu J H, Sun X and Wang J M 2013 *J. Mod. Opt.* **60** 1598
[22] Bonod N and Neáuport J 2006 *Opt. Commun.* **260** 649
[23] Neauport J, Lavastre E, Razé G, Dupuy G, Bonod N, Balas M, Villele G de, Flamand J, Kaladgew S and Desserouer F 2007 *Opt. Express* **15** 12508
[24] Golberg D E 1989 *Genetic Algorithms in Search, Optimization, and Machine Learning*, Addison-Wesley
[25] Kong W J, Zhang W F, Yun M J, Liu J H, Sun X and Wang W 2012 *J. Mod. Opt.* **59** 1680
[26] Blair P, Taghizadeh M R, Parkes W and Wilkinson C D W 1995 *Appl. Opt.* **34** 2406
[27] Zhang G P, Ming H, Xie J P and Ye J X 1997 *Chin. J. Las.* **A24** 699